

Data-driven discovery of multiscale chemical reactions governed by the law of mass action

Juntao Huang¹ Yizhou Zhou² Wen-An Yong³

Abstract

In this paper, we propose a method to discover multiscale chemical reactions governed by the law of mass action from data. First, we use one matrix to represent the stoichiometric coefficients for both the reactants and products in a system without catalysis reactions. The negative entries in the matrix denote the stoichiometric coefficients for the reactants and the positive ones denote the products. Second, we find that the conventional optimization methods usually get stuck in the local minima and could not find the true solution in learning multiscale chemical reactions. To overcome this difficulty, we propose to perform a round operation on the stoichiometric coefficients which are closed to integers and do not update them in the afterwards training. With such a treatment, the dimension of the searching space is greatly reduced and the global minima is eventually obtained. Several numerical experiments including the classical Michaelis–Menten kinetics and the hydrogen oxidation reactions verify the good performance of our algorithm in learning multiscale chemical reactions. The code is available at <https://github.com/JuntaoHuang/multiscale-chemical-reaction>.

Key Words: Chemical Reactions; Multiscale; Machine Learning; Nonlinear Regression; Ordinary Differential Equations

¹Department of Mathematics, Michigan State University, East Lansing, MI 48824, USA. E-mail: huangj75@msu.edu

²Department of Mathematical Sciences, Tsinghua University, Beijing, China. E-mail: zhouyz16@mails.tsinghua.edu.cn

³Department of Mathematical Sciences, Tsinghua University, Beijing, China. E-mail: way-ong@tsinghua.edu.cn

1 Introduction

Chemical reactions are fundamental in many scientific fields including biology, environment, material science, chemical engineering and so on. To identify the reactions from experimental data, the traditional methods are mainly based on some empirical laws and expert knowledge [6]. Recently, thanks to the rapid development of machine learning [12], it is desirable to develop a data-driven method which aims at finding the underlying chemical reactions from massive data automatically.

Consider a reaction system with n_s species participating in n_r reactions:



for $i = 1, 2, \dots, n_r$. Here \mathcal{S}_k is the chemical symbol for the k -th species, the nonnegative integers ν'_{ik} and ν''_{ik} are the stoichiometric coefficients of the k -th species in the i -th reaction, and k_{if} and k_{ir} are the direct and reverse reaction rates of the i -th reaction. The reaction is reversible if both k_{if} and k_{ir} are positive. Denote by $u_k = u_k(t)$ the concentration of the k -th species at time t . According to the law of mass action, the evolution of u_k obeys the ordinary differential equations (ODEs) [17]

$$\frac{du_k}{dt} = \sum_{i=1}^{n_r} (\nu''_{ik} - \nu'_{ik}) \left(k_{if} \prod_{j=1}^{n_s} u_j^{\nu'_{ij}} - k_{ir} \prod_{j=1}^{n_s} u_j^{\nu''_{ij}} \right). \quad (1.1)$$

Given the concentration time series data $\{(u_k(t_n), u'_k(t_n)), k = 1, \dots, n_s, n = 1, \dots, N\}$, our goal is to learn the stoichiometric coefficients ν'_{ik}, ν''_{ik} and reaction rate constants k_f and k_r . Realistically, often only $u_k(t_n)$ is available, and the time derivatives $u'_k(t_n)$ could be approximated using numerical differentiations [18, 4].

There are already some works on this topic. In [8], the authors extend the sparse identification of nonlinear dynamics (SINDy) method [3] to vector-valued ansatz functions, each describing a particular reaction process. However, the approach relies on expert knowledge, which precludes the application in a new reaction system with unknown reaction pathways.

Within the framework of SINDy, other works are [2, 1, 15]. In order to improve the performance of SINDy, two additional steps including least-squares regression and stepwise regression in the identification are introduced in [2], which are based on the traditional statistical methods. In [1], SINDy is combined with deep neural networks (DNNs) to adaptively model and control the process dynamics. An implicit-SINDy is proposed and applied to infer Michaelis-Menten enzyme kinetics in [15]. Additionally, the authors proposed a statistical learning framework based on group-sparse regression which leverage prior knowledge from physical principles in [14]. For example, the mass conservation is enforced in the JAK-STAT reaction pathway for signal transduction. Our work is mainly motivated by [9], where the authors proposed a Chemical Reaction Neural Network (CRNN) by resorting to the feature of the equations in (1.1). The parameters in CRNN correspond to the stoichiometric coefficients and rate constants of the chemical reactions and the network has only one hidden layer with the exponential activation functions.

Different from CRNN in [9], we use only one matrix of order $n_r \times n_s$ to represent the stoichiometric coefficients for both the forward and reverse reactions by assuming no catalysis reactions. The negative entries in the matrix denote the stoichiometric coefficients for the reactants and the positive ones denote the products.

Here, an essential difficulty is that the rate constants often differ in a wide range of magnitude. This usually causes the stiffness of the chemical reactions. To provide some insights into this difficulty, we design a nonlinear regression problem to fit a polynomial with two terms, see (2.1) in Section 2. The given coefficients of the polynomial differ in several orders of magnitudes and the polynomial degree is to be determined. We find numerically that the conventional optimization algorithm usually gets stuck in the local minima and could not find the true solution. But we observe that the learned polynomial degree of the terms with larger coefficient is close to the true solution. Motivated by this observation, we propose to freeze the parameters which are close to integer in the optimization process if the loss function does

not decrease. The revised algorithm works well for this problem. Some theoretical analysis is also provided to explain the numerical phenomenon.

We then generalize the technique of freezing integer parameters to learn the multiscale chemical reactions. We propose to freeze the stoichiometric coefficients which are close to integers in the optimization process. More specifically, if the loss function does not decrease in the training, we perform a round operation on the stoichiometric coefficients which are closed to integers and do not update them in the afterwards training. With such a treatment, the dimension of the searching space is greatly reduced. Several numerical experiments including the classical Michaelis–Menten kinetics and the hydrogen oxidation reactions verify that our method performs much better in learning stiff chemical reactions.

This paper is organized as follows. In Section 2, we investigate a multiscale nonlinear regression problem numerically and theoretically. Our algorithm for learning the multiscale chemical reactions is presented in Section 3. In Section 4, the performance of the algorithm is validated through several numerical examples. Finally, conclusions and the outlook of future work are presented in Section 5.

2 Multiscale nonlinear regression problem

To provide some insights into the difficulties in learning the multiscale chemical reactions, we consider a nonlinear regression problem to fit the following scalar function:

$$y = f(x; \boldsymbol{\theta}) = f(x; \theta_1, \theta_2) = c_1 x^{\theta_1} + c_2 x^{\theta_2}. \quad (2.1)$$

Here c_1 and c_2 are two given constants satisfying $|c_1| \ll |c_2|$, and $\boldsymbol{\theta} := (\theta_1, \theta_2) \in \mathbb{Z}^2$ are integers to be determined. This simple toy model captures two essential features of the multiscale chemical reactions. The first feature is that the right-hand side of the chemical reaction ODEs (1.1) is polynomial and the stoichiometric coefficients must be integer. The second one is that the multiscale chemical reactions often have reaction rates which differ in several orders of

magnitudes.

Assume that the data is given by $\mathcal{D} = \{(x_i, y_i) : i = 1, \dots, N\}$. To estimate the integer pair $\boldsymbol{\theta}$, we define the loss function to be the mean squared error (MSE):

$$\mathcal{L}(\boldsymbol{\theta}) = \frac{1}{N} \sum_{i=1}^N (f(x_i; \boldsymbol{\theta}) - y_i)^2. \quad (2.2)$$

Next, conventional optimization methods can be used to obtain the estimation of $\boldsymbol{\theta}$.

In the numerical experiment, we take $c_1 = 1$, $c_2 = 100$. The ground truth solutions are $\theta_1 = 1$ and $\theta_2 = 2$. The data x_i for $i = 1, \dots, N$ is randomly sampled from a uniform distribution in $(0, 1)$ with the number of data $N = 1000$, and $y_i = c_1 x_i + c_2 x_i^2$. To reduce possible stochastic effects introduced by the mini-batch gradient descent, we use the full batch gradient decent. The learning rate is taken to be 10^{-4} . The Adam optimization method [11] is applied here. The initial guess of θ_1 and θ_2 is randomly chosen in $(-1, 1)$.

For this toy model, we numerically find that the naive implementation will get stuck in the local minima $(\theta_1, \theta_2) = (3.8286, 1.9745)$ and could not find the true solution. The history of the loss function and the parameters θ_1 and θ_2 in the training are presented in Figure 2.1, see the dashed lines.

Although the naive optimization could not find the global minima, we notice that $\theta_2 = 1.9745$ in this local minima is close to the true solution $\theta_2 = 2$. Motivated by this observation, we propose to freeze the parameters which are close to integer if the optimization get stuck into the local minima. To be more specifically, we record the history of the loss function in the training. If the loss function does not decrease, we check the parameters θ_1 and θ_2 : if any of these is close to its nearest integer with a given threshold, we round it to the nearest integer and do not update it in the afterwards optimization process.

For comparison, we also plot the history of the loss function and the parameters with the technique of freezing integer parameters in Figure 2.1, see the solid lines. The threshold is taken to be 0.05 in this test. The loss stops decreasing with the epoch around 7000. Then θ_2

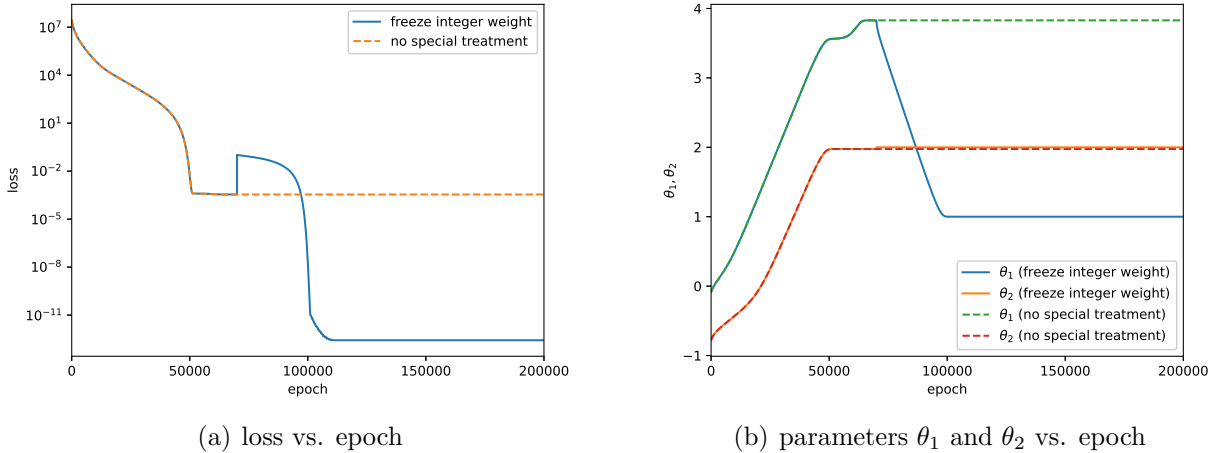


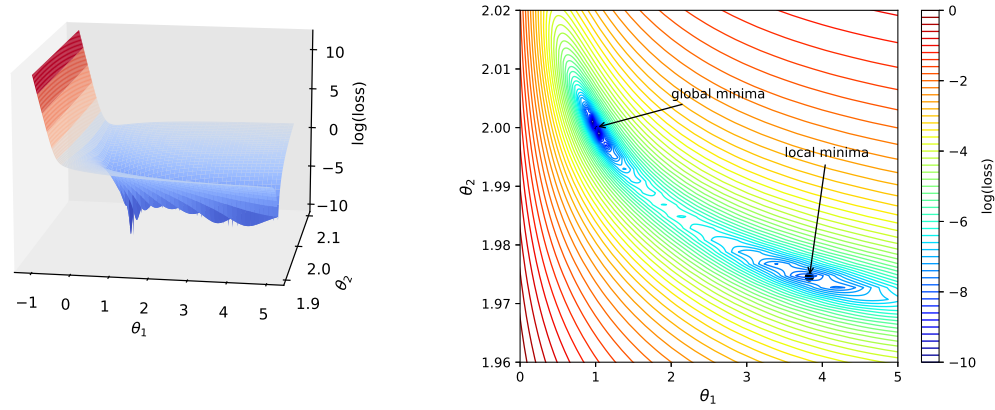
Figure 2.1: Multiscale nonlinear regression problem: the history of loss function and the parameters θ_1 and θ_2 , comparison of freeze the integer parameters and without this treatment

is rounded to 2 and only θ_1 is updated afterwards. The true solution is eventually obtained when the epoch is around 10000.

To better understand why the method without any special treatment is easy to get stuck in the local minima, we investigate the landscape of the loss function. In Figure 2.2, we plot the 3D surface and the contour map for the loss as a function of $\theta = (\theta_1, \theta_2)$. In Figure 2.2 (a), it is observed that the loss function has several local minima in which θ_2 is close to 2. Moreover, the local minima $(\theta_1, \theta_2) = (3.8286, 1.9745)$ in the naive implementation is also labeled in Figure 2.2 (b).

We also plot the profiles of the loss function with fixed $\theta_2 = 1.99, 2$ and 2.01 in Figure 2.3. It is observed that slight perturbations in θ_2 have a considerable impact on the minima of the loss function. Moreover, the loss as a 1D function with fixed $\theta_2 = 2$ is well-behaved. This explains why our algorithm is easy to find the global minima after freezing the integer parameter θ_2 .

We mention that we also test other cases with different coefficients c_1 and c_2 satisfying $|c_2/c_1| = 10^3, 10^4, 10^5$ and different integers θ_1 and θ_2 . The results are similar and thus



(a) loss function surface plot

(b) loss function contour map

Figure 2.2: Multiscale nonlinear regression problem: loss function landscape. Left: loss function surface plot (in log scale); right: loss function contour map (in log scale), local minima $(\theta_1, \theta_2) = (3.8286, 1.9745)$.

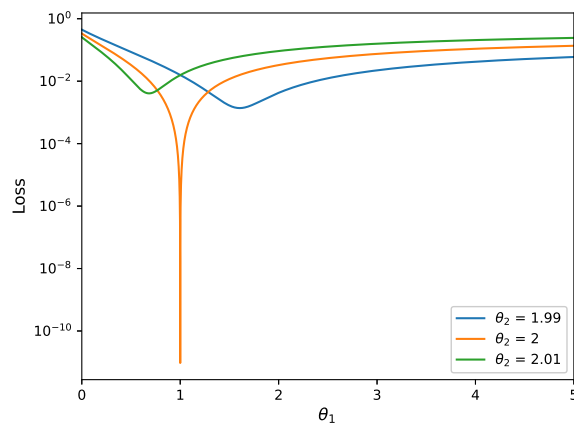


Figure 2.3: Multiscale nonlinear regression problem: loss function with fixed $\theta_2 = 1.99, 2$ and 2.01 .

omitted here.

We conclude this section with some theoretical analysis to explain the local minima phenomenon observed in the numerical experiment. By taking gradient of the loss function in (2.2), we have

$$\frac{\partial \mathcal{L}}{\partial \theta_j} = c_j \frac{2}{N} \sum_{i=1}^N (c_1(x_i^{\theta_1} - x_i^{\theta_1^e}) + c_2(x_i^{\theta_2} - x_i^{\theta_2^e})) x_i^{\theta_j} \ln x_i, \quad j = 1, 2. \quad (2.3)$$

Here θ_i^e denotes the true solution of the parameter θ_i for $i = 1, 2$. From the gradient (2.3), we can provide some insights on the phenomenon that the local minima θ_2 is close to the true solution θ_2^e . To reach the local minima, the gradient (2.3) should be zero. Thus, the term $(c_1(x_i^{\theta_1} - x_i^{\theta_1^e}) + c_2(x_i^{\theta_2} - x_i^{\theta_2^e}))$ in (2.3) should be close to zero. Since $|c_1| \ll |c_2|$, this constraint is satisfied if θ_2 is close to θ_2^e but θ_1 is not necessarily close to θ_1^e .

3 Algorithm for learning multiscale reactions

In this section, we present our algorithm for learning multiscale chemical reactions (1.1). First, by assuming the non-existence of catalysis reactions, we use a matrix to represent the stoichiometric coefficients for both the reactants and the products. Each row of the matrix represents one reaction, where the negative items denote the stoichiometric coefficients for the reactants and the positive ones for the products. In addition, to overcome the difficulties in learning multiscale chemical reactions, we generalize the technique of freezing integer parameters in the multiscale nonlinear regression problem in Section 2.

Given the concentration time series data $\{(u_k(t_n), u'_k(t_n)), k = 1, \dots, n_s, n = 1, \dots, N\}$, our goal is to learn the stoichiometric coefficients and the reaction rate constants. To better illustrate the algorithm, we firstly introduce some vector notations. We denote the forward and reverse reaction rates in (1.1) by $\mathbf{k}_f = (k_{1f}, k_{2f}, \dots, k_{n_r f})^T$, $\mathbf{k}_r = (k_{1r}, k_{2r}, \dots, k_{n_r r})^T$ and

the stoichiometric coefficients in (1.1) are collected in two matrices:

$$\mathbf{V}' = \begin{pmatrix} \nu'_{11} & \nu'_{12} & \cdots & \nu'_{1n_s} \\ \nu'_{21} & \nu'_{22} & \cdots & \nu'_{2n_s} \\ \vdots & \vdots & \ddots & \vdots \\ \nu'_{n_r1} & \nu'_{n_r2} & \cdots & \nu'_{n_r n_s} \end{pmatrix}, \quad \mathbf{V}'' = \begin{pmatrix} \nu''_{11} & \nu''_{12} & \cdots & \nu''_{1n_s} \\ \nu''_{21} & \nu''_{22} & \cdots & \nu''_{2n_s} \\ \vdots & \vdots & \ddots & \vdots \\ \nu''_{n_r1} & \nu''_{n_r2} & \cdots & \nu''_{n_r n_s} \end{pmatrix}. \quad (3.1)$$

We assume that there exist no catalysis reactions where catalyst presents in both reactants and products. Mathematically, this is equivalent to the fact that the two matrices \mathbf{V}' and \mathbf{V}'' do not have the same indices for the non-zero elements. In this case, the matrix $\mathbf{V} = (\nu_{ik}) := \mathbf{V}'' - \mathbf{V}'$ satisfies

$$\nu_{ik} = \begin{cases} \nu''_{ik}, & \text{if } \nu_{ik} \geq 0, \\ -\nu'_{ik}, & \text{if } \nu_{ik} < 0. \end{cases}$$

According to this property, we only need to pin down the matrix \mathbf{V} , and then \mathbf{V}' and \mathbf{V}'' are determined by $\nu''_{ik} = \max(0, \nu_{ik})$ and $\nu'_{ik} = -\min(0, \nu_{ik})$.

Next, we define the neural network $\mathcal{N} = \mathcal{N}(u_1, \dots, u_{n_s}) : \mathbb{R}^{n_s} \rightarrow \mathbb{R}^{n_s}$ which has the input $\mathbf{u} := (u_1, \dots, u_{n_s})^T$ and the parameters $\mathbf{l}_f = (l_{1f}, l_{2f}, \dots, l_{n_r f})^T$, $\mathbf{l}_r = (l_{1r}, l_{2r}, \dots, l_{n_r r})^T$ and \mathbf{V} :

$$\mathcal{N}(u_1, \dots, u_{n_s})_k = \sum_{i=1}^{n_r} \nu_{ik} \left(\exp(l_{if}) \prod_{j=1}^{n_s} u_j^{-\min(0, \nu_{ik})} - \exp(l_{ir}) \prod_{j=1}^{n_s} u_j^{\max(0, \nu_{ik})} \right)$$

for $k = 1, \dots, n_s$. Here the parameters l_{if} and l_{ir} denotes the logarithm of the reaction rates k_{if} and k_{ir} [9]. This change of variable has two advantages. The first one is that the positivity of the reaction rates is guaranteed automatically. The second one is that the reaction rates for multiscale chemical reactions usually differ in several orders of magnitudes. The slight changes of l_{if} and l_{ir} will make k_{if} and k_{ir} change a lot, which could potentially make the neural network to be more robust in the training process.

The loss function is defined as the mean squared error (MSE) between the data for the time derivatives and the output of the neural network:

$$\mathcal{L} = \frac{1}{N} \sum_{n=1}^N \sum_{k=1}^{n_s} (\mathcal{N}(u_1(t_n), \dots, u_{n_s}(t_n))_k - u'_k(t_n))^2 + \lambda \mathcal{L}_r. \quad (3.2)$$

Here $\lambda \mathcal{L}_r$ is the regularization term with λ the regularization constant. Both L_1 and L_2 regularization terms are included here:

$$\mathcal{L}_r = \sum_{i=1}^{n_r} \sum_{k=1}^{n_s} |\nu_{ik}| + \sum_{i=1}^{n_r} \sum_{k=1}^{n_s} \nu_{ik}^2. \quad (3.3)$$

This neural network works quite well for non-stiff chemical reactions. However, for stiff reactions, we observe that the optimization usually gets stuck in the local minima in the training process and could not find the true solution. The common techniques such as the mini-batch and reducing the learning rate do not work in such case. To attack this problem, we generalize the technique of freezing integer weight in nonlinear regression problem in Section 2.

The training procedure is split into two parts. The first part is to learn the weight matrix \mathbf{V} . To better illustrate the algorithm, we introduce some notation. Denote the vector in the j -th row of \mathbf{V} by \mathbf{v}_j for $j = 1, \dots, n_r$, and define the distance to the nearest integer for any vector $\mathbf{v} \in \mathbb{R}^d$ as

$$d_{\text{int}}(\mathbf{v}) := \|\mathbf{v} - \lfloor \mathbf{v} \rfloor\|_{\infty} = \max_{i \in \{1, \dots, d\}} |v_i - \lfloor v_i \rfloor| \quad (3.4)$$

where $\lfloor \cdot \rfloor$ denotes the function rounding an arbitrary real number to the nearest integer and it is defined to work element-wise on vectors. We keep track of the loss function in the training process. If the loss function stops decreasing, we check if any row of \mathbf{V} is close to the nearest integers, i.e., $d_{\text{int}}(\mathbf{v}_j) \leq \epsilon$. Here, $\epsilon > 0$ is a hyperparameter and we take $\epsilon = 0.05$ in all the numerical tests. If the j -th row of \mathbf{V} satisfies the condition $d_{\text{int}}(\mathbf{v}_j) \leq \epsilon$, then we round \mathbf{v}_j to $\lfloor \mathbf{v}_j \rfloor$ and do not update it in the afterwards training. Moreover, to help the optimization algorithm escape from local minima, we randomly reinitialize other non-integer elements in \mathbf{V} . After all the elements in \mathbf{V} reach integer, we freeze them and then learn the parameters \mathbf{l}_f and \mathbf{l}_r related to the reaction rates. We remark that in this part in learning reaction rates, the SINDy algorithms [3, 8] can also be applied here. The algorithm is illustrated in Algorithm 1.

Remark 3.1. Here we assume that the reactions are all reversible. However, the algorithm

can be also applied to irreversible reactions without any modification. The expected result is that the learned reverse reaction rate for the irreversible reactions will be close to zero. This will be demonstrated numerically in Example 4.2 in Section 4.

Algorithm 1: Training procedure for chemical reactions

Input : time series data $\{(u_k(t_n), u'_k(t_n)), k = 1, \dots, n_s, n = 1, \dots, N\}$
Output: stoichiometric coefficient matrix \mathbf{V} , chemical reaction rates \mathbf{k}_f and \mathbf{k}_r

- 1 initialize hyperparameters: total number of epoch N , learning rate lr , regularization coefficient λ , check integer frequency M , integer threshold ϵ ;
- 2 initialize parameters: \mathbf{V} , \mathbf{l}_f and \mathbf{l}_r ;
 // step 1: learning V
- 3 $L_{\text{rec}} = \text{numpy.zeros}(N)$; // record loss function in each epoch
- 4 $S_{\text{int}} = []$; // store index of reaction whose weights are close to integer
- 5 **for** $i = 1, \dots, N$ **do**
- 6 | Compute loss \mathcal{L} ;
- 7 | Compute $\frac{\partial \mathcal{L}}{\partial \theta}$ by backpropagation ;
- 8 | Update parameters by Adam methods ;
 // if loss increase, then check if any row of V is close to integer
- 9 | **if** $i \equiv 0 \pmod{M}$ and $L_{\text{rec}}[i] \geq L_{\text{rec}}[i - 1]$ **then**
- 10 | | **for** $j = 1, \dots, n_s$ **do**
- 11 | | | **if** $d_{\text{int}}(\mathbf{v}_j) \leq \epsilon$ **then**
- 12 | | | | $S_{\text{int}}.append(j)$;
- 13 | | | | $\mathbf{v}_j \leftarrow \lfloor \mathbf{v}_j \rfloor$;
- 14 | | | **end**
- 15 | | | **if** $j \notin S_{\text{int}}$ **then**
- 16 | | | | $\mathbf{v}_j \leftarrow \text{rand}(-2, 2)$; // random reinitialize non-integer weights
- 17 | | | **end**
- 18 | | **end**
- 19 | **end**
 // if all the reactions weights are integers, then stop learning V
- 20 | **if** $S_{\text{int}} = \{1, \dots, n_r\}$ **then**
- 21 | | **break**;
- 22 | **end**
- 23 **end**
 // step 2: learning k_f and k_r
- 24 **for** $i = 1, \dots, N$ **do**
- 25 | Compute loss \mathcal{L} ;
- 26 | Compute $\frac{\partial \mathcal{L}}{\partial \theta}$ by backpropagation ;
- 27 | Update parameters θ (excluding \mathbf{V}) by Adam methods ;
- 28 **end**
- 29 **for** $i = 1, \dots, n_r$ **do**
- 30 | $k_{if} \leftarrow \exp(l_{if})$;
- 31 | $k_{ir} \leftarrow \exp(l_{ir})$;
- 32 **end**

4 Numerical results

In this section, the performance of our algorithm will be investigated in three examples. The first example is an artificial reaction mechanism with two reactions [13]. The second one is the well-known Michaelis–Menten kinetics [10] in biochemistry. The third one is the hydrogen oxidation reactions [7, 5].

In all the numerical tests, the learning rate is taken to be 10^{-3} . The regularization coefficient is 10^{-8} . The integer threshold is 0.05. The total epoch number is 10^6 and we check integer weights every 10^4 epoch. The mini-batch gradient descent is applied with the batch size 10. The data is generated by solving the governing ODEs numerically using implicit Runge-Kutta method of the Radau IIA family of the fifth order [20] with small enough tolerance. The code is available at <https://github.com/JuntaoHuang/multiscale-chemical-reaction>.

In all the numerical examples, we randomly take 100 different initial conditions to generate the data. For each initial condition, we take uniform time snapshots at $t_n = n\Delta t$ with $n = 0, \dots, 10$ and $\Delta t = 0.1$. The datasets are randomly split into the training datasets and the validation datasets by a ratio of 4:1. It is worthy to note that here we do not take Δt to be too small so that the datasets could be potentially replaced by the experiment data in the future.

Example 4.1 (hypothetical stiff reaction network). The first test case is an artificial reaction network with two reactions, taken from [13]:



Here F, R and P indicate fuel, radical and product in combustions, respectively. The reaction rates are taken to be $k_1^+ = k_1^- = 1$ and $k_2^+ = k_2^- = 10^3$. The two reversible reactions in (4.1) have dramatically different rate constants. Thus, the second reaction (4.1b) will quickly

approach to equilibrium after a transient period, after which the first one (4.1a) becomes rate-limiting.

The corresponding ODE system for (4.1) is linear. The eigenvalues of the coefficient matrix are $\lambda_1 = -2000$, $\lambda_2 = -1.5$ and $\lambda_3 = 0$, which differ in several orders of magnitudes. This indicates that the ODE system is stiff.

To illustrate the advantage of the freezing integer weights technique, we compare the performance of the algorithm with and without this special treatment. The history of training and validation errors is shown in Figure 4.4. The relative error stays around 10^{-3} without this technique, and decrease to 10^{-6} after using this technique. The learned parameters are shown in Table 4.1. The upper part of the table is the learned parameters with the freezing integer weights technique, which agrees well with the ground truth in (4.1). By contrast, the algorithm without imposing this technique could not generate the correct result. Moreover, it is interesting to see that the learned first reaction and the second one has the stoichiometric coefficients with opposite sign. We also notice that the summation of the forward rate k_f of the first reaction and the reverse rate k_r of the second one is close to the true reaction rate 10^3 . This indicates that the effect of these two learned reactions is identical to the fast reaction (4.1b) and the slow reaction (4.1a) is not captured here. This is similar to the phenomenon we observed in the multiscale nonlinear regression in Section 2.

freezing	x_1	x_2	x_3	k_f	k_r
1	0.000	1.000	-1.000	1.000e+03	1.000e+03
2	-1.000	1.000	0.000	1.000e+00	1.000e+00
no freezing	x_1	x_2	x_3	k_f	k_r
1	-0.001	0.999	-0.999	7.448e+02	5.731e+02
2	0.000	-0.999	0.999	4.277e+02	2.559e+02

Table 4.1: Example 4.1: learned parameters, with the freezing integer weight and without special treatment. Here (x_1, x_2, x_3) denotes the row vector of the weight matrix \mathbf{V} .

In our algorithm, the number of chemical reactions is a hyperparameter to be determined. Next, we test the algorithm with different number of chemical reactions. We take the number

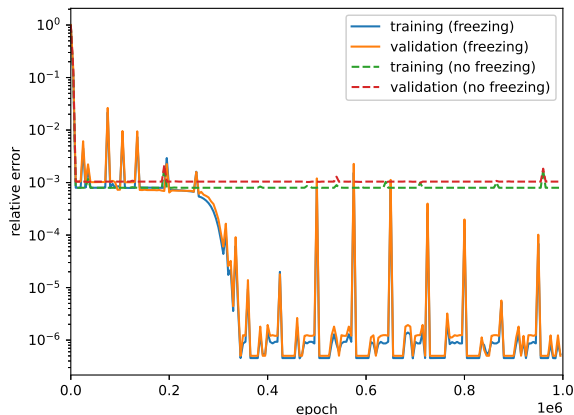


Figure 4.4: Example 4.1: the history of the relative error for the training data and the verification data. Solid line: freezing the integer weights; dashed line: without special treatment.

of reactions range from 1 to 4 and the relative error in the training data and the validation data is shown in Figure 4.5. The relative error decreases by three magnitudes when increasing the number of proposed reactions from one to two and reaches a plateau after that. It then can be inferred that the kinetics could be well described using two reactions. The learned parameters with different number of reactions are listed in Table 4.2. With only one reaction, the algorithm can only discover the fast reaction (4.1b) well. With overestimated reaction number, the learned parameters have stoichiometric coefficients or reaction rates which are close to zero.

Example 4.2 (enzyme kinetics). In this example, we consider Michaelis–Menten kinetics [10], one of the best-known models of enzyme kinetics in biochemistry. It involves an enzyme, E, binding to a substrate, S, to form a complex, ES, which in turn releases a product, P, regenerating the original enzyme. This can be represented schematically as [10]



Here k_f denotes the forward rate constant, k_r the reverse rate constant, and k_{cat} the catalytic rate constant. This model is used in a variety of biochemical situations other than

reaction num 1	x_1	x_2	x_3	k_f	k_r
1	0.000	-1.000	1.000	1.000e+03	1.000e+03
reaction num 2	x_1	x_2	x_3	k_f	k_r
1	0.000	1.000	-1.000	1.000e+03	1.000e+03
2	-1.000	1.000	0.000	1.000e+00	1.000e+00
reaction num 3	x_1	x_2	x_3	k_f	k_r
1	0.000	1.000	-1.000	1.000e+03	1.000e+03
2	-1.000	1.000	0.000	9.217e+02	1.218e+02
3	0.750	-0.101	0.384	7.887e-04	1.813e-03
reaction num 4	x_1	x_2	x_3	k_f	k_r
1	0.000	-1.000	1.000	1.000e+02	1.000e+02
2	0.000	0.000	0.000	5.931e+01	5.929e+01
3	0.000	0.000	0.000	2.526e+01	2.524e+01
4	1.000	-1.000	0.000	1.000e+00	1.000e+00

Table 4.2: Example 4.1: learned parameters with different number of reactions. Here (x_1, x_2, x_3) denotes the row vector of the weight matrix \mathbf{V} .

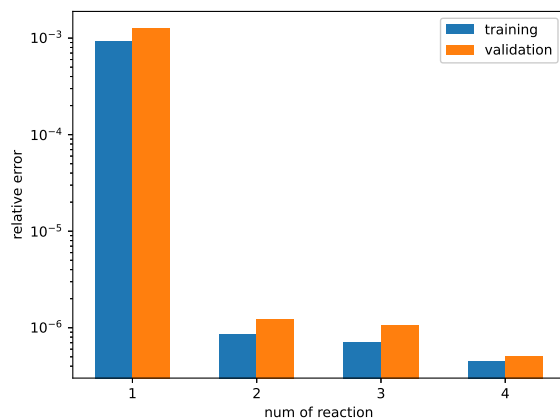


Figure 4.5: Example 4.1: relative error for training data and verification data with different number of reactions.

enzyme-substrate interaction, including antigen–antibody binding, DNA–DNA hybridization, and protein–protein interaction [16]. Moreover, the rate constants values vary widely between different enzymes. In our test case, we follow [19] and take $k_f = 10^6$, $k_r = 10^3$ and $k_{cat} = 10$.

Note that the second reaction in (4.2) is not reversible. Here, we also apply the same algorithm without any modification. The results with and without the technique of freezing integer weights are listed in Table 4.3. In the upper part of the table, the reverse rate for the second reaction is 1.949×10^{-4} . It then can be inferred that the system could be well described using two reactions with the second one to be irreversible. Again, the algorithm without this treatment could only get the correct result for the first faster reaction in (4.2). The evolution of the loss function is similar to that in Example 4.1 and thus omitted here.

freezing	x_1	x_2	x_3	x_4	k_f	k_r
1	−1.000	−1.000	1.000	0.000	1.000e+06	1.000e+03
2	1.000	0.000	−1.000	1.000	1.000e+01	1.949e-04
no freezing	x_1	x_2	x_3	x_4	k_f	k_r
1	−0.999	−0.999	0.989	0.000	9.921e+05	9.929e+02
2	−1.001	−1.000	2.385	0.000	7.956e+03	1.392e+01

Table 4.3: Example 4.2: learned parameters, with the freezing integer weight and without special treatment. Here (x_1, x_2, x_3, x_4) denotes the row vector of the weight matrix \mathbf{V} .

We also investigate the performance of the algorithm with different number of reactions. The relative error for the training and validation data is presented in Table 4.6. Again, the error decrease a lot when increasing number of reactions from one to two. This indicates that two reactions are enough to describe the kinetics.

Example 4.3 (hydrogen oxidation reaction). In this example, we consider a model for hydrogen oxidation reaction where six species H_2 (hydrogen), O_2 (oxygen), H_2O (water), H , O , OH (radicals) are involved in six steps in a closed system under constant volume and temperature

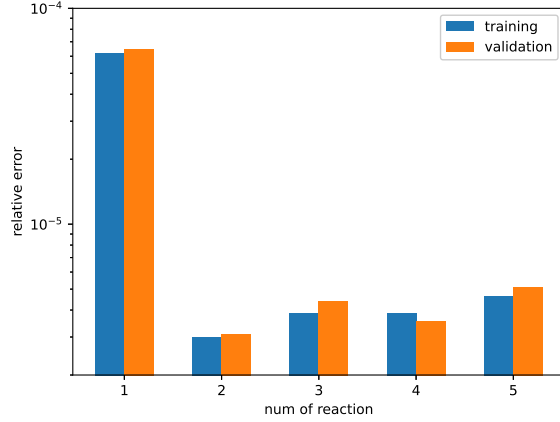
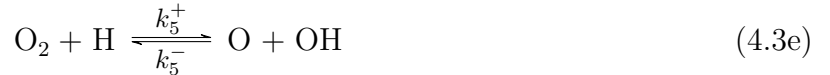


Figure 4.6: Example 4.2: relative error for training data and verification data with different number of reactions.

[7, 5]:



with the reaction rates $k_1^+ = 2$, $k_2^+ = k_3^+ = 1$, $k_4^+ = k_5^+ = 1 \times 10^3$, $k_1^- = 1 \times 10^2$, $k_1^- = 2.16 \times 10^2$, $k_2^- = 3.375 \times 10^2$, $k_3^- = 1.4 \times 10^3$, $k_4^- = 1.08 \times 10^4$, $k_5^- = 3.375 \times 10^4$, $k_6^- = 7.714285714285716 \times 10^{-1}$. The system (4.3) is fictitious in the sense that the subset of equations corresponds to the simplified picture of this chemical process and the rate constants reflect only orders of magnitude for relevant real-world systems. The magnitude of the reaction rates vary from 10^{-1} to 10^4 , which make the chemical reaction very stiff and difficult to learn from data.

We first compare the performance of our algorithm with and without the freezing integer

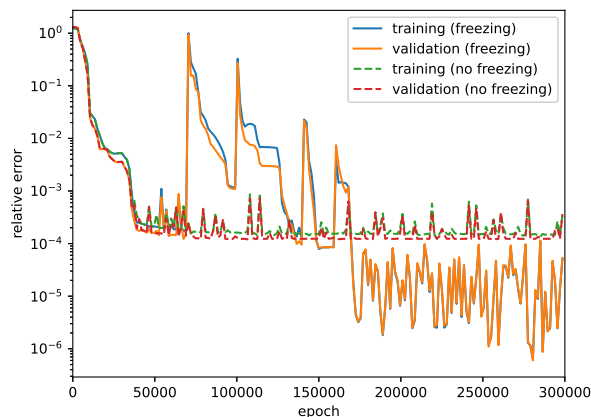


Figure 4.7: Example 4.3: the history of the relative error for the training data and the verification data. Solid line: freezing the integer weights; dashed line: without special treatment.

weight treatment. The history of the training and the verification error is shown in Figure 4.7. Again, we observe that this technique greatly reduces the training and the validation error. The learned parameters are listed in Table 4.4. The algorithm can generate the correct result with this technique. Without using this technique,

We also test the performance of the algorithm with Gaussian noise. The algorithm can get the correct prediction of the stoichiometric coefficients with the noise level 10^{-4} and 10^{-3} . The reaction rates are shown in Table 4.5. The relative errors for reaction rates are typically less than the order of 10^{-2} for 10^{-3} noise and 10^{-3} for 10^{-4} noise.

Moreover, we plot the evolution of the concentration of the six species with the noise level 10^{-3} in Figure 4.9. We observe good agreement of the solution generated by our learned model and the exact solution. We also measure the prediction error of the learned model at 100 uniformly points in the time interval $[0, 10]$. The prediction errors are 1.953×10^{-6} with zero noise, 9.152×10^{-4} with noise level 10^{-4} and 8.710×10^{-4} with noise level 10^{-3} .

freezing	x_1	x_2	x_3	x_4	x_5	x_6	k_f	k_r
1	0.000	1.000	0.000	1.000	-1.000	-1.000	3.375e+04	1.000e+03
2	1.000	0.000	0.000	-1.000	1.000	-1.000	1.080e+04	1.000e+03
3	0.000	0.000	1.000	-1.000	0.000	-1.000	1.400e+03	1.000e+00
4	0.000	1.000	0.000	0.000	-2.000	0.000	3.375e+02	1.000e+00
5	1.000	0.000	0.000	-2.000	0.000	0.000	2.160e+02	2.000e+00
6	-1.000	0.000	1.000	0.000	-1.000	0.000	1.000e+02	7.714e-01
no freezing	x_1	x_2	x_3	x_4	x_5	x_6	k_f	k_r
1	0.000	0.938	0.000	0.923	-1.000	-1.001	1.971e+04	5.512e+02
2	0.000	1.087	0.000	1.108	-0.999	-0.999	1.407e+04	4.488e+02
3	0.885	0.000	0.115	-1.000	0.885	-1.000	1.217e+04	2.112e+01
4	-1.004	0.000	0.087	0.910	-1.008	0.913	1.077e+03	2.926e+01
5	0.000	0.996	0.008	0.000	-1.997	0.000	3.379e+02	8.912e-01
6	0.987	0.000	0.007	-1.984	0.004	0.004	2.170e+02	3.377e+00

Table 4.4: Example 4.3: learned parameters, with the freezing integer weight and without special treatment. Here $(x_1, x_2, x_3, x_4, x_5, x_6)$ denotes the row vector of the weight matrix \mathbf{V} . The negative sign means the reactant and the positive sign means the product.

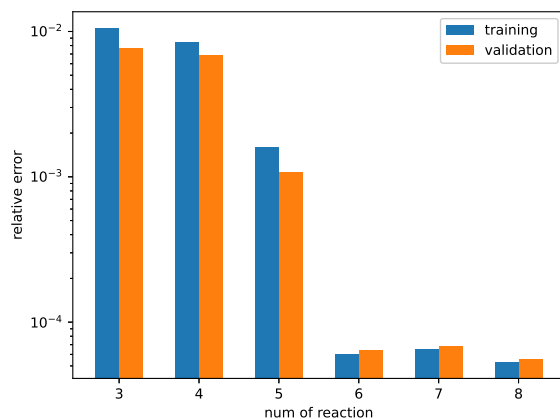


Figure 4.8: Example 4.3: relative error for training data and verification data with different number of reactions.

noise 10^{-3}	\hat{k}_f	relative error	\hat{k}_r	relative error
1	3.375e+04	5.706e-05	1.002e+03	2.097e-03
2	1.080e+04	2.789e-04	1.001e+03	1.374e-03
3	1.399e+03	4.413e-04	9.631e-01	3.836e-02
4	3.399e+02	7.103e-03	9.235e-01	8.278e-02
5	2.161e+02	6.927e-04	2.130e+00	6.107e-02
6	9.764e+01	2.417e-02	8.047e-01	4.137e-02
noise 10^{-4}	\hat{k}_f	relative error	\hat{k}_r	relative error
1	3.375e+04	6.482e-06	1.000e+03	2.099e-04
2	1.080e+04	2.803e-05	1.000e+03	1.379e-04
3	1.400e+03	4.491e-05	9.963e-01	3.707e-03
4	3.377e+02	7.161e-04	9.923e-01	7.717e-03
5	2.160e+02	6.965e-05	2.013e+00	6.469e-03
6	9.976e+01	2.366e-03	7.748e-01	4.294e-03

Table 4.5: Example 4.3: learned reaction rates with noise.

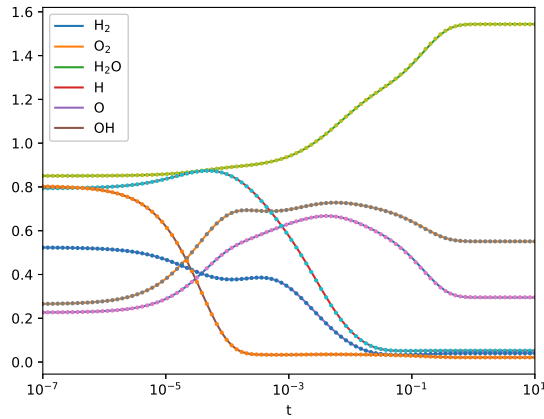


Figure 4.9: Example 4.3: the evolution of the concentration of the 6 species in the hydrogen oxidation reaction problem obtained by solving the original ODEs (4.3) and our learned ODEs. noise level 10^{-3} .

5 Conclusion

In this paper, we propose a method to discover multiscale chemical reactions governed by the law of mass action from data. The method mainly contains two novel points. First, we use one matrix to represent the stoichiometric coefficients for both the reactants and products in a system without catalysis reactions. The negative entries in the matrix denote the stoichiometric coefficients for the reactants and the positive ones denote the products. Second, by considering a nonlinear regression problem, we find that the conventional optimization methods usually get stuck in the local minima and could not find the true solution in learning multiscale chemical reactions. To escape from the local minima, we propose to perform a round operation on the stoichiometric coefficients which are closed to integers and do not update them in the afterwards training. With such a treatment, the dimension of the searching space is greatly reduced and the global minima is eventually obtained. The performance of the algorithm is investigated with several numerical experiments including the classical Michaelis–Menten kinetics and the hydrogen oxidation reactions.

There are still some problems to be addressed in order to develop a robust and general framework for discovering multiscale chemical reactions from data. We shall highlight some of the challenges that could guide future advances. First, it is interesting to generalize the technique of freezing integer parameters to the catalysis reactions. Second, the reaction rates are changing in many chemical reaction systems. For example, the temperature dependence follows the Arrhenius Law. The performance of our algorithm remains to be investigated in these scenarios.

References

- [1] B. Bhadriraju, M. S. F. Bangi, A. Narasingam, and S. I. Kwon. Operable adaptive sparse identification of systems (oasis): application to chemical processes. *AIChE Journal*,

- 66(11):e16980, 2020.
- [2] B. Bhadriraju, A. Narasingam, and J. S.-I. Kwon. Machine learning-based adaptive model identification of systems: Application to a chemical process. *Chemical Engineering Research and Design*, 152:372–383, 2019.
- [3] S. L. Brunton, J. L. Proctor, and J. N. Kutz. Discovering governing equations from data by sparse identification of nonlinear dynamical systems. *Proceedings of the national academy of sciences*, 113(15):3932–3937, 2016.
- [4] R. Chartrand. Numerical differentiation of noisy, nonsmooth data. *ISRN Applied Mathematics*, 2011, 2011.
- [5] E. Chiavazzo and I. V. Karlin. Quasi-equilibrium grid algorithm: Geometric construction for model reduction. *Journal of Computational Physics*, 227(11):5535–5560, 2008.
- [6] C. W. Gao, J. W. Allen, W. H. Green, and R. H. West. Reaction mechanism generator: Automatic construction of chemical kinetic mechanisms. *Computer Physics Communications*, 203:212–225, 2016.
- [7] A. N. Gorban and I. V. Karlin. *Invariant manifolds for physical and chemical kinetics*, volume 660. Springer Science & Business Media, 2005.
- [8] M. Hoffmann, C. Fröhner, and F. Noé. Reactive sindy: Discovering governing reactions from concentration data. *The Journal of Chemical Physics*, 150(2):025101, 2019.
- [9] W. Ji and S. Deng. Autonomous discovery of unknown reaction pathways from data by chemical reaction neural network. *arXiv preprint arXiv:2002.09062*, 2020.
- [10] J. P. Keener and J. Sneyd. *Mathematical physiology*, volume 1. Springer, 1998.

- [11] D. P. Kingma and J. Ba. Adam: A method for stochastic optimization. *arXiv preprint arXiv:1412.6980*, 2014.
- [12] Y. LeCun, Y. Bengio, and G. Hinton. Deep learning. *nature*, 521(7553):436–444, 2015.
- [13] T. Lu and C. K. Law. On the applicability of directed relation graphs to the reduction of reaction mechanisms. *Combustion and Flame*, 146(3):472–483, 2006.
- [14] S. Maddu, B. L. Cheeseman, C. L. Müller, and I. F. Sbalzarini. Learning physically consistent mathematical models from data using group sparsity. *arXiv preprint arXiv:2012.06391*, 2020.
- [15] N. M. Mangan, S. L. Brunton, J. L. Proctor, and J. N. Kutz. Inferring biological networks by sparse identification of nonlinear dynamics. *IEEE Transactions on Molecular, Biological and Multi-Scale Communications*, 2(1):52–63, 2016.
- [16] D. L. Nelson, A. L. Lehninger, and M. M. Cox. *Lehninger principles of biochemistry*. Macmillan, 2008.
- [17] H. G. Othmer. Analysis of complex reaction networks. *Lecture Notes, School of Mathematics, University of Minnesota*, 2003.
- [18] L. I. Rudin, S. Osher, and E. Fatemi. Nonlinear total variation based noise removal algorithms. *Physica D: nonlinear phenomena*, 60(1-4):259–268, 1992.
- [19] V. Srinivasan and R. Aiken. Stage-wise parameter estimation for stiff differential equations. *AIChE journal*, 32(2):195–199, 1986.
- [20] G. Wanner and E. Hairer. *Solving ordinary differential equations II*. Springer Berlin Heidelberg, 1996.